Opto-Electronic Advances

Supplementary information

2022, Vol. 5, No. 12

DOI: 10.29026/oea.2022.210159

Graphene photodetector employing double slot structure with enhanced responsivity and large bandwidth

Siqi Yan[1,2]*, Yan Zuo[1,2], Sanshui Xiao[1], Leif Katsuo Oxenløwe[1] and Yunhong Ding[1]*

[1]DTU Electro, Department of Electrical and Photonics Engineering, Technical University of Denmark, Kgs. Lyngby DK-2800, Denmark; [2]School of Optical and Electronic Information and Wuhan National Laboratory for Optoelectronics, Huazhong University of Science and Technology, Wuhan 430074, China.

*Correspondence: SQ Yan, E-mail: siqya@mail.hust.edu.cn; YH Ding, E-mail: yudin@fotonik.dtu.dk

This file includes:

Supplementary information for this paper is available at https://doi.org/10.29026/oea.2022.210159

Section 1: Theoretical analysis of the double slot structure

COMSOL Multiphysics is used to analyze the graphene absorption coefficient and the metallic Ohmic absorption of the double slot structure. The cross-section view and the geometry parameters of the theoretical model of are shown in Fig. S1.

In the calculation, the graphene monolayer is described as a surface current model. The surface conductivity of graphene is modeled as the equation below:

$$\sigma\left(\omega,\mu_{\mathrm{c}},\Gamma,T\right)=\frac{-\mathrm{j}e^{2}}{\pi\hbar^{2}(\omega+\mathrm{j}2\Gamma)}\int_{0}^{\infty}\zeta\left(\frac{\partial f_{\mathrm{d}}(\zeta)}{\partial\zeta}-\frac{\partial f_{\mathrm{d}}(-\zeta)}{\partial\zeta}\right)\mathrm{d}\zeta+\frac{\mathrm{j}(\omega+\mathrm{j}2\Gamma)}{\pi\hbar^{2}}\int_{0}^{\infty}\zeta\left(\frac{f_{\mathrm{d}}(-\zeta)-f_{\mathrm{d}}(\zeta)}{(\omega+\mathrm{j}2\Gamma)^{2}-4(\zeta/\hbar)^{2}}\right)\mathrm{d}\zeta\ , \quad \text{(S1)}$$

In Eq. (1), the first term represents intraband contributions while the second term represents interband contributions. Moreover, $f_{\mathrm{d}}\left(\zeta\right)=\left(\mathrm{e}^{(\zeta-\mu_{\mathrm{c}})/k_{\mathrm{B}}T}+1\right)^{-1}$ is the Fermi-Dirac distribution. ω is the angular frequency of the photon. Γ represents the scattering rate. μ_{c} is the chemical potential of graphene. T is the temperature. e is the electron charge. $\hbar$ is the reduced Plank constant, and k_{B} is the Boltzmann constant. Refractive indices for the materials involved are set as n_{Si}=3.45, n_{SiO2}=1.45, n_{Al2O3}=1.746. The permittivities of gold and titanium are $\varepsilon_{\mathrm{Au}}=-93.069+11.108*\mathrm{i}$ and $\varepsilon_{\mathrm{Ti}}=2.0696+21.391*\mathrm{i}$, respectively. The graphene absorption coefficient $\alpha_{\mathrm{graphene}}$ (dB/μm) is calculated by the equation below:

$$\alpha_{\mathrm{graphene}}=4.343{*}10^{-6}*\frac{1}{2}\mathrm{Re}\left(\sigma_{\mathrm{g}}\right)\left(\left|\boldsymbol{E}_{x}\right|^{2}+\left|\boldsymbol{E}_{z}\right|^{2}\right)/\iint P\left(x,y\right)\mathrm{d}x\mathrm{d}y\ , \quad \text{(S2)}$$

where Re(σ_{g}) is the real part of the graphene conductivity, $\boldsymbol{E}_{x}$ and $\boldsymbol{E}_{z}$ is the x and z direction component of the electric fields along the graphene surface of the transmitted mode within the double slot structure. $P\left(x,y\right)$ represents the average power at the coordinate (x,y) of the simulated waveguide. The overall loss α_{mode} (dB/μm) of the double slot structure could be calculated by the equation below:

$$\alpha_{\mathrm{mode}}=4.343*10^{-6}*2k_{0}*\mathrm{Im}\left(n_{\mathrm{eff}}\right)\ , \quad \text{(S3)}$$

where k_{0} is the propagation constant and n_{eff} is the effective refractive index of the mode. Therefore, the metallic absorption $\alpha_{\mathrm{metallic}}$ (dB/μm) is calculated by the difference of α_{mode} and $\alpha_{\mathrm{graphene}}$:

$$\alpha_{\mathrm{metallic}}=\alpha_{\mathrm{mode}}-\alpha_{\mathrm{graphene}}\ . \quad \text{(S4)}$$

The coupling between the double slot structure and the silicon slot structure is realized by inverse-tapering the Au metal to minimize the coupling loss[S1]. In our design, the length of the coupling region is 500 nm, giving a coupling loss of 2.17 dB per side measured by the cut-back method. Higher coupling efficiency could be achieved by a longer taper length, but at the sacrifice of a larger device footprint.

Section 2: Experiment setups of the static and dynamic response measurement

The experiment setup of the static response measurement is shown in Fig. S2. An erbium-doped fiber amplifier (EDFA) first amplifies the light emitted from the laser. Then the variable optical attenuator (VOA) is placed between the polariz-

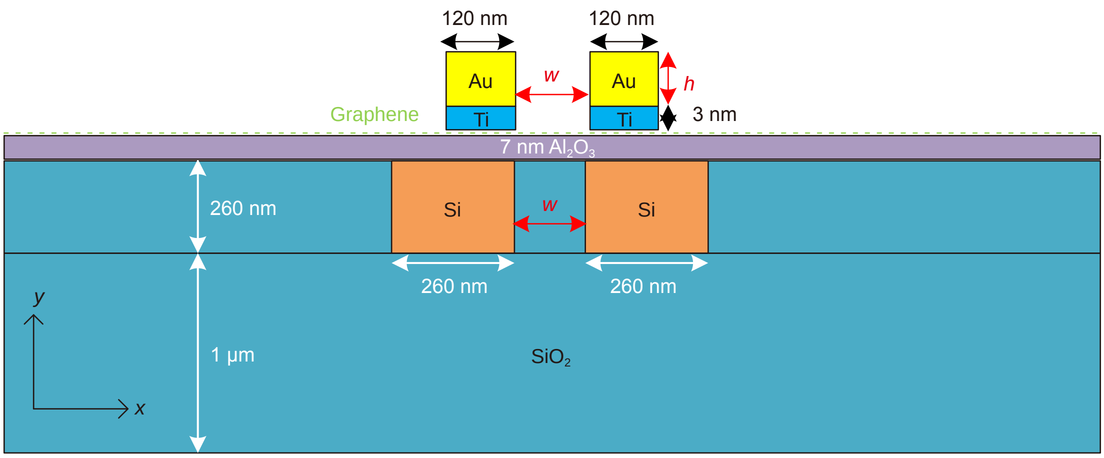

Fig. S1 | The cross-section view and the geometric parameters of the simulated double slot structure.

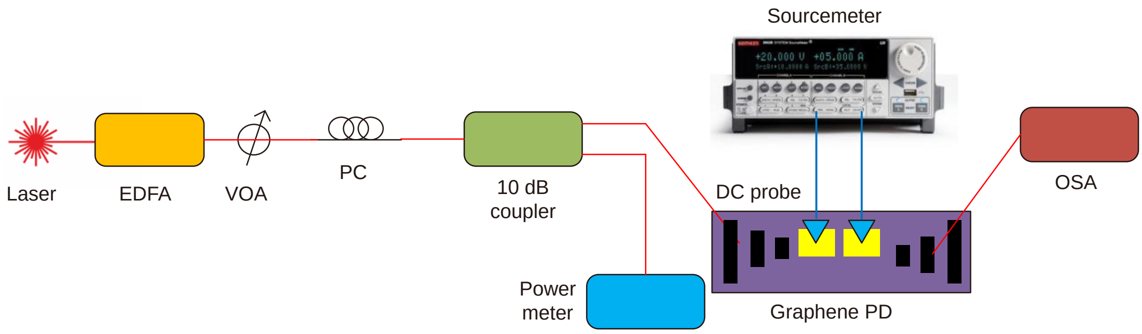

Fig. S2 | Experiment setup of the static response measurement.

ation controller (PC) and the EDFA to adjust the input optical power into the chip while the power meter is used to measure the optical power. The input optical signal is coupled from the single mode fiber (SMF) to the silicon waveguide by a grating coupler. External bias voltage provided by a sourcemeter (Keithley 2600B) is applied on the graphene PD through two direct current (DC) probes contacted on the metal pad of the chip. When the laser is switched on and off, the current with and without light injection is recorded by the sourcemeter as I_0 and I_1, respectively. The photocurrent (I_{pc}) is defined as the difference between I_1 and I_0, i.e. $I_{pc}= I_1-I_0$. The power of the light reaching the detection region (P_{real}) could be calculated by the relation below:

$$P_{\text{real}} = P_0 - \alpha_{\text{couplingloss}} \;, \tag{S5}$$

where P_0 is the optical power measured by the power meter and $\alpha_{\text{couplingloss}}$ is the sum of the loss of both grating coupler and the strip to slot mode converter. Then the responsivity (R) could be calculated as:

$$R = \frac{I_{\text{pc}}}{P_{\text{real}}} \;. \tag{S6}$$

Due to bandwidth limitation of 40 GHz, the vector network analyzer (VNA) (model: HEWLETT-PACKARD P8722C) is used to obtain the frequency response under 40 GHz. As the Fig. S3 shows, the optical signal from laser is modulated by the output RF signal of VNA through an intensity modulator and then amplified by the EDFA. The PC is used to control the polarization state of the input light. Radio-frequency (RF) probe is used to conduct the RF signal detected by the graphene PD out to the RF Cable. The Bias Tee (model: SHF BT 65C) is used to connect VNA, sourcemeter and the RF probe as the Fig. S3 displays.

To obtain the device's frequency response higher than 40 GHz, we used the experimental setup shown in Fig. S4. Similar to the methods reported in our previous work[S2], we use the combination of a signal generator (model: Agilent E8267D), a phase modulator (model: EOspace PM-DV3-40-PFA-PFA-LV) and a waveshaper (model: FINISAR Waveshaper 4000s) to generate optical signal with high frequency RF signal. The frequency beating signals from 30 GHz to 90 GHz were generated by adjusting the signal generator and the waveshaper. Then the optical signal is amplified by the

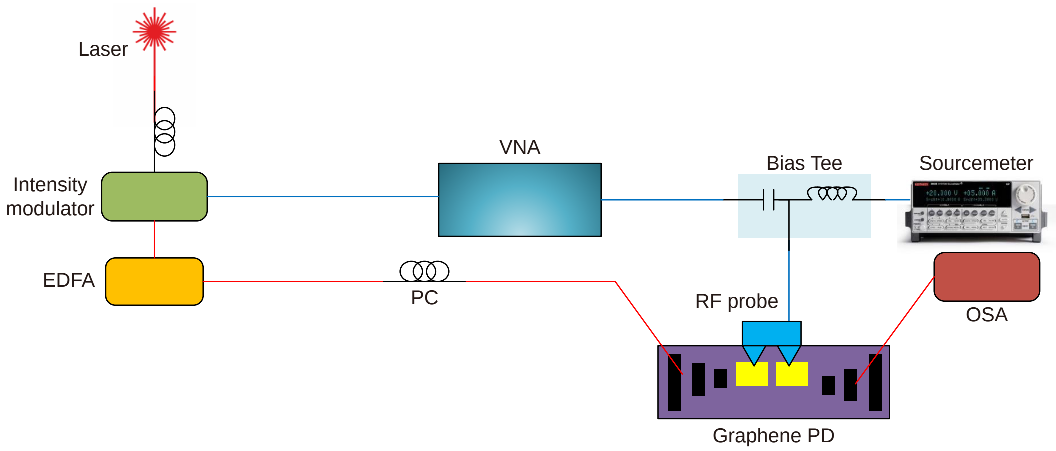

Fig. S3 | Experiment setup of the dynamic response measurement with VNA.

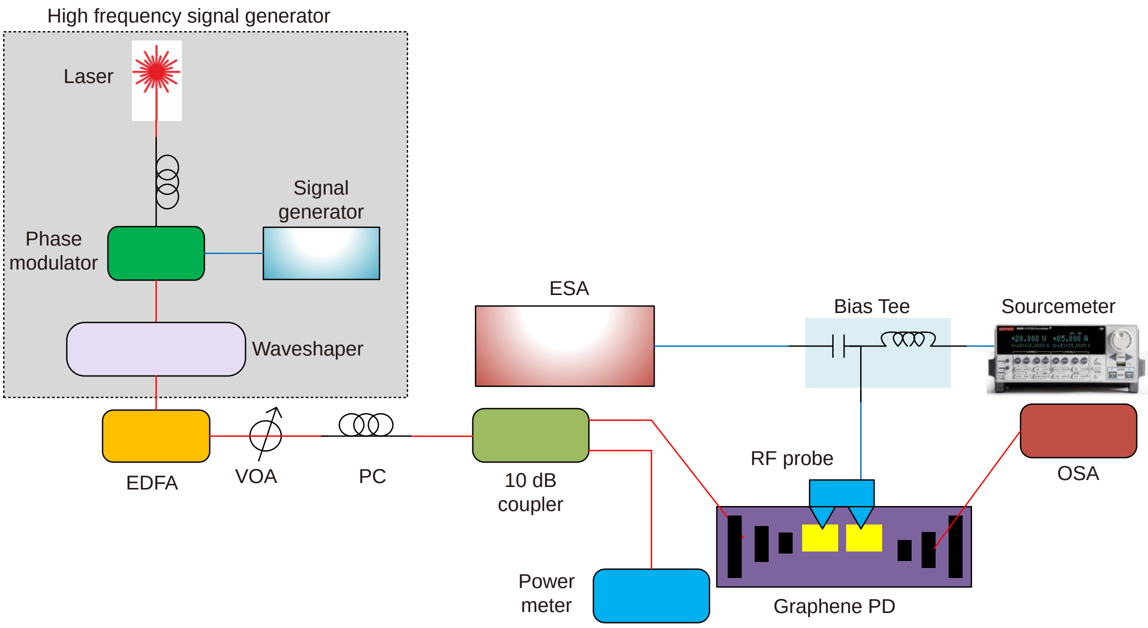

Fig. S4 | Experiment setup of the dynamic response with ESA.

EDFA. To ensure the power of the RF signal injected into the chip remain constant during the adjustment, VOA and power meter are used to monitor the optical power during the adjustment. At last, the RF signal detected by the graphene PD is injected to the electrical spectrum analyzer (model: Anritsu MS2760A) to measure its peak power.

At last, a modulated NRZ-OOK optical signal is injected to the chip to test its performance as a receiver. As the Fig. S5 shows, the NRZ-OOK optical signal is generated by an intensity modulator driven by a bit pattern generator (model: Adsantec PRBS45). Before the detected signal is injected to the oscilloscope (model: Agilent Infiniium DCA 86100B, with Agilent 86118A Remote Sampling Module 70 GHz), it is amplified by an electrical broadband preamplifier (model: Picosecond 5830, DC-15 GHz). Since the upper bandwidth limitation of 15 GHz of the electrical amplifier, the bit rate of the detected signal is limited to the 15 Gbit/s.

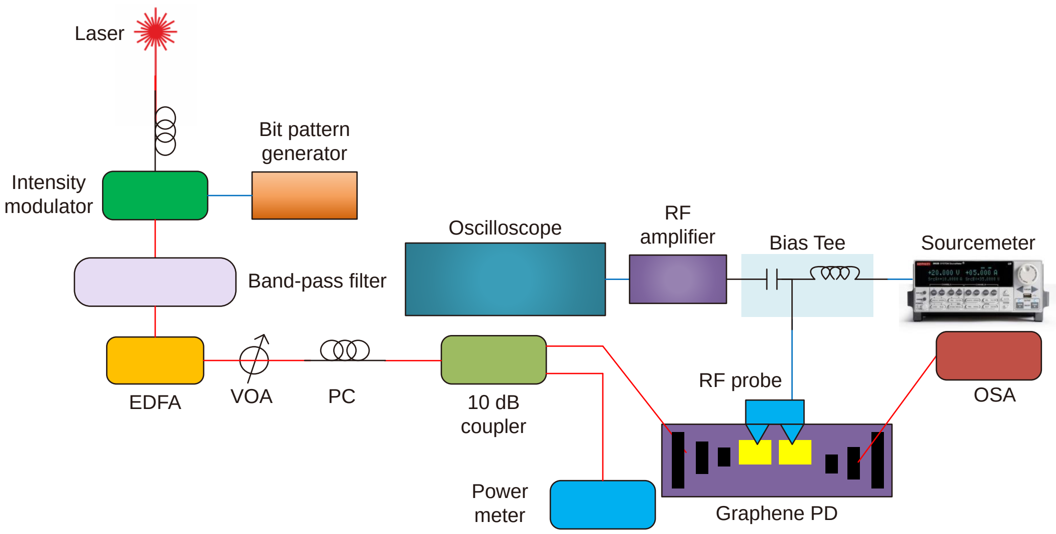

Fig. S5 | Experiment setup of graphene PD as a receiver.

References

S1. Ono M, Taniyama H, Xu H, Tsunekawa M, Kuramochi E et al. Deep-subwavelength plasmonic mode converter with large size reduction for Si-wire waveguide. *Optica* **3**, 999–1005 (2016).

S2. Ding YH, Cheng Z, Zhu XL, Yvind K, Dong JJ et al. Ultra-compact integrated graphene plasmonic photodetector with bandwidth above 110 GHz. *Nanophotonics* **9**, 317–325 (2020).